

SSSAJ

Soil Science Society of America Journal



SOIL SCIENCE SOCIETY OF AMERICA JOURNAL

Business and Editorial Offices at
677 South Segoe Road, Madison, WI 53711
(www.soils.org)

SOIL SCIENCE EDITORIAL BOARD

Editorial Board, SSSA

WARREN A. DICK, *Editor-in-chief*
R.L. MULVANEY, *Editor*

Technical editors

D.E. RADCLIFFE (Div. S-1)	J.W. BAUDER (Div. S-6)
G. MULLINS (Div. S-4, S-8)	L.M. SHUMAN (Div. S-2)
M.J. VEPRASKAS	D. MYROLD
(Div. S-5, S-9, S-10)	(Div. S-3, S-7)

Associate Editors

F.J. ADAMSEN	R. HORTON	J.P. SCHMIDT
C. AMRHEIN	C.-H. HUANG	C.P. SCHULTHESS
J.C. BELL	C.E. JOHNSON	J.C. SEAMAN
J.L. BOETTINGER	C.T. JOHNSTON	J.S. SELKER
S.A. BOYD	D.A. LAIRD	F.J. SIKORA
K.F. BRONSON	R.E. LAMOND	R.J. SOUTHARD
N. CAVALLARO	F.J. LEIJ	J.S. STROCK
J.D. CHOROVER	D. LINDBO	A.A. SZOGI
J.E. COMPTON	S.D. LOGSDON	T.L. THOMPSON
S.M. DABNEY	L. MA	H.A. TORBERT
T.H. DAO	A.P. MALLARINO	F.T. TURNER
R.P. DICK	E.L. MCCOY	C. VAN KESSEL
J.A. ENTRY	P.A. MCDANIEL	H. VAN MIEGROET
M.E. ESSINGTON	K. MCINNES	M.G. WAGGER
C.V. EVANS	L.E. MOODY	M. WANDER
T.R. FOX	L.A. MORRIS	L.T. WEST
A.J. FRANZLUEBBERS	E.A. NATER	B.J. WIENHOLD
P.M. GALE	J.R. NIMMO	L. WU
C.J. GANTZER	Y.A. PACHEPSKY	D.R. ZAK
S.R. GOLDBERG	G.S. PETTYGROVE	
E.A. GUERTAL	T.J. SAUER	

N.H. RHODEHAMEL, *managing editor*
nrhodehamel@agronomy.org
D.M. KRAL, *associate executive vice president*
REBECCA MALLEY, *assistant editor*
rmalley@agronomy.org
CARRIE J. CZERWONKA, *assistant editor*
cczerwonka@agronomy.org

2002 Officers of SSSA

JOHN W. DORAN, <i>President</i> USDA-ARS, Univ. of Nebraska Lincoln, NE	R.J. LUXMOORE, <i>Past-President</i> Oak Ridge National Laboratory Oak Ridge, TN
M.J. SINGER, <i>President-elect</i> Dep. Land, Air, and Water Resources University of California Davis, CA	

Published bimonthly by the Soil Science Society of America, Inc. Periodicals postage paid at Madison, WI, and at additional mailing offices.

Postmaster: Send address change to *SSSA Journal*, 677 S. Segoe Rd., Madison, WI 53711.

Subscription rates (nonmember): \$247 per year, within the USA; all others \$277. Single copies, \$30 USA; elsewhere, \$36. Members are eligible for reduced subscription rates. New subscriptions, renewals, and new memberships that include the *SSSA Journal* begin with the first issue of the current year. Claims for copies lost in the mail must be received within 90 days of publication date for domestic subscribers, and within 26 weeks of publication date for foreign subscribers.

Membership in the Society is not a requirement for publication in *SSSA Journal*; however, nonmembers will be charged an additional amount for the first six published pages of a manuscript. To qualify for member rates, at least one author must be an active, emeritus, graduate student, or undergraduate student member of SSSA, CSSA, or ASA on the date the manuscript is accepted for publication.

Volunteered papers will be assessed a charge of \$25 per page for nonmembers for each printed page from page one through page six; a charge of \$190 per page (\$95 per half page) will be assessed all papers for additional pages. No charge will be assessed against invited review papers or comments on matters having to do with soil science. The Society absorbs the cost of reproducing illustrations up to \$15 for each paper.

Contributions to the *SSSA Journal* may be (i) papers and notes on original research; and (ii) "Comments and Letters to the Editor" containing (a) critical comments on papers published in one of the Society outlets or elsewhere, (b) editorial comments by Society officers, or (c) personal comments on matters having to do with soil science. Letters to the Editor are limited to one printed page. Contributions need not have been presented at annual meetings. Original research findings are interpreted to mean the outcome of scholarly inquiry, investigation, or experimentation having as an objective the revision of existing concepts, the development of new concepts, or the improvement of techniques in some phase of soil science. Short, critical reviews or essays on timely subjects, upon invitation by the Editorial Board, may be published on a limited basis. Refer to SSSA Publication Policy (Soil Sci. Soc. Am. J. 64(1):1-3, 2000) and to the *Publications Handbook and Style Manual* (ASA-CSSA-SSSA, 1998).

Keep authors anonymous from reviewers by listing title, author(s), author-paper documentation, and acknowledgments on a detachable title page. Repeat manuscript title on the abstract page.

Manuscripts are to be sent to Dr. Richard L. Mulvaney, Editor, *SSSA Journal*, University of Illinois, 1102 South Goodwin Avenue, Urbana, IL 61801 (email: mulvaney@uiuc.edu). Four copies of the manuscript on line-numbered paper are required. All other correspondence should be directed to the Managing Editor, 677 S. Segoe Rd., Madison, WI 53711.

Trade names are sometimes listed in papers in this journal. No endorsement of these products by the publisher is intended, nor is any criticism implied of similar products not mentioned.

Copyright © 2002 by the Soil Science Society of America, Inc. Permission for printing and for reprinting the material contained herein has been obtained by the publisher. Other users should request permission from the author(s) and notify the publisher if the "fair use" provision of the U.S. Copyright Law of 1976 (P.L. 94-553) is to be exceeded.

Division S-1—Soil Physics

- 673–685 Inversion of Soil Conductivity Profiles from Electromagnetic Induction Measurements: Theory and Experimental Verification. *J.M.H. Hendrickx, B. Borchers, D.L. Corwin, S.M. Lesch, A.C. Hilgen-dorf, and J. Schlue*
- 686–695 Measured and Predicted Solute Leaching from Multiple Undisturbed Soil Columns. *S.D. Logsdon, K.E. Keller, and T.B. Moorman*
- 696–701 Prediction of Dispersivity for Undisturbed Soil Columns from Water Retention Parameters. *E. Perfect, M.C. Sukop, and G.R. Haszler*
- 702–709 Effect of Water Regime on Aggregate-tensile Strength, Rupture Energy, and Friability. *Lars J. Munkholm and Bev D. Kay*
- 710–721 Vapor Flow to Horizontal Wells in Unsaturated Zones. *Hongbin Zhan and Eungyu Park*
- 722–727 Moisture Effects on Soil Reflectance. *David B. Lobell and Gregory P. Asner*
- 728–734 Evaluation of the OhmMapper Instrument for Soil Moisture Measurement. *Jeffrey P. Walker and Paul R. Houser*
- 735–743 Horizontal and Vertical TDR Measurements of Soil Water Content and Electrical Conductivity. *Arie Nadler, S.R. Green, I. Vogeler, and B.E. Clothier*
- 744–752 Three-region Campbell Model for Unsaturated Hydraulic Conductivity in Undisturbed Soils. *T.G. Poulsen, P. Moldrup, B.V. Iversen, and O.H. Jacobsen*
- 753–759 Spatial and Statistical Similarities of Local Soil Water Fluxes. *Bing Cheng Si*
- 760–773 Imaging Fluorescent Dye Concentrations on Soil Surfaces: Uncertainty of Concentration Estimates. *Jan Vanderborght, Paul Gähwiler, Hannes Wydler, Ute Schultze, and Hannes Flüher*
- 774–787 Identification of Transport Processes in Soil Cores Using Fluorescent Tracers. *Jan Vanderborght, Paul Gähwiler, and Hannes Flüher*
- 788–796 Measurement of Attenuation and Speed of Sound in Soils. *Michael L. Oelze, William D. O'Brien, Jr., and Robert G. Darmody*

Division S-2—Soil Chemistry

- 797–804 Desorption Kinetics of Cadmium²⁺ and Lead²⁺ from Goethite: Influence of Time and Organic

Acids. *Leslie J. Glover II, Matthew J. Eick, and Patrick V. Brady*

- 805–817 Comparison of Redox Indicators in a Paddy Soil during Rice-Growing Season. *S. Gao, K.K. Tanji, S.C. Scardaci, and A.T. Chow*
- 818–825 Kinetics of Arsenic Adsorption on Goethite in the Presence of Sorbed Silicic Acid. *Catherine A. Waltham and Matthew J. Eick*

Division S-3—Soil Biology & Biochemistry

- 826–833 Dynamics of a Soil Microbial Community under Spring Wheat. *Søren O. Petersen, Pamela S. Frohne, and Ann C. Kennedy*
- 834–844 Temperature and Moisture Effects on Nitrification Rates in Tropical Rain-Forest Soils. *Lutz Breuer, Ralf Kiese, and Klaus Butterbach-Bahl*

Division S-3—Notes

- 845–847 Maize Root-Induced Change in Soil Organic Carbon Pools. *B.C. Liang, X.L. Wang, and B.L. Ma*

Division S-4—Soil Fertility & Plant Nutrition

- 848–856 Management Effects on Barley Straw Decomposition, Nitrogen Release, and Crop Production. *M.H. Beare, P.E. Wilson, P.M. Fraser, and R.C. Butler*
- 857–867 Yield and Soil Fertility Trends in a 20-Year Rice–Wheat Experiment in Nepal. *A.P. Regmi, J.K. Ladha, H. Pathak, E. Pasuquin, C. Bueno, D. Dawe, P.R. Hobbs, D. Joshy, S.L. Maskey, and S.P. Pandey*
- 868–877 Sequential Phosphorus Extraction of a ³³P-Labeled Oxisol under Contrasting Agricultural Systems. *S. Buehler, A. Oberson, I.M. Rao, D.K. Friesen, and E. Frossard*

Division S-5—Pedology

- 878–887 Pedogenesis of Vesicular Horizons, Cima Volcanic Field, Mojave Desert, California. *K. Anderson, S. Wells, and R. Graham*
- 888–896 Brazil's Soil Carbon Stocks. *Martial Bernoux, Maria da Conceição Santana Carvalho, Boris Volkoff, and Carlos Clemente Cerri*

Continued on page ii

This issue's cover: A surface crust of various soil types: clayey, kaolinitic (top), clayey, non-phyllsilicate (bottom), clayey, montmorillonitic (middle right), and sandy loam, montmorillonitic (middle left). Please see 'Soil Mineralogy and texture effects on crust micromorphology, infiltration, and erosion' by I.I.C. Wakindiki and M. Ben-Hur, p. 897–905.

Division S-6—Soil & Water Management & Conservation

- 897–905 Soil Mineralogy and Texture Effects on Crust Micromorphology, Infiltration, and Erosion. *I.I.C. Wakindiki and M. Ben-Hur*
- 906–912 Tillage, Nitrogen, and Cropping System Effects on Soil Carbon Sequestration. *Ardell D. Halvorson, Brian J. Wienhold, and Alfred L. Black*
- 913–923 Root Length Growth of Eight Crop Species in Haplustoll Soils. *Stephen D. Merrill, Donald L. Tanaka, and Jonathan D. Hanson*
- 924–930 Cultivation-Induced Effects on Belowground Biomass and Organic Carbon. *N. Slobodian, K. Van Rees, and D. Pennock*
- 931–938 Eastern Gamagrass Root Penetration in Adverse Subsoil Conditions. *Rachel E. Gilker, Ray R. Weil, Donald T. Krizek, and Bahram Momen*
- 939–947 Manganese Distribution and Patterns of Soil Wet-ting and Depletion in a Piedmont Hillslope. *D.K. Cassel, M.M. Afyuni, and W.P. Robarge*
- 948–958 Soil Quality in Mediterranean Mountain Environ-ments: Effects of Land Use Change. *M. Sánchez-Marañón, M. Soriano, G. Delgado, and R. Delgado*

Division S-7—Forest & Range Soils

- 959–968 Soil Analyses as Indicators of Phosphorus Re-sponse in Young Eucalypt Plantations. *Daniel S. Mendham, Philip J. Smethurst, Greg K. Holz, Robert C. Menary, Tim S. Grove, Chris Weston, and Tom Baker*
- 969–978 Soil Organic Matter Dynamics in the Subhumid Agroecosystems of the Ethiopian Highlands: Evi-dence From Natural ^{13}C Abundance and Particle-

- Size Fractionation. *D. Solomon, F. Fritzsche, J. Lehmann, M. Tekalign, and W. Zech*
- 979–987 Abiotic Nitrogen Uptake in Semiarid Grassland Soils of the U.S. Great Plains. *J.E. Barrett, D.W. Johnson, and I.C. Burke*

Division S-8—Nutrient Management & Soil & Plant Analysis

- 988–998 Development of Reflectance Spectral Libraries for Characterization of Soil Properties. *Keith D. Shepherd and Markus G. Walsh*
- 999–1007 Pathways of Soil Phosphorus Transformations after 8 Years of Cultivation under Contrasting Cropping Practices. *Zhiming Zheng, Régis R. Si-mard, Jean Lafond, and Léon E. Parent*

Division S-8—Notes

- 1008–1011 A Technique to Facilitate Diffusions for Nitro-gen-Isotope Analysis by Direct Combustion. *K.K. Moran, R.L. Mulvaney, and S.A. Khan*

2001 Meeting Reports and Minutes

- 1012–1014 SSSA Headquarters Report, 2001
- 1014–1021 SSSA Executive Committee Meetings
- 1022–1024 SSSA Board of Directors Meetings
- 1024 Presidents of the SSSA
- 1025–1050 Reports of SSSA Divisions, Branches, and Com-mittees, 2001
- 1051–1060 SSSA Fellows of the Soil Science Society of Amer-ica Elected in 2001
- 1061–1071 Soil Science Research Awards, 2001
- 1072–1074 SSSA Fellows and Award Recipients
- 1075–1082 SSSA Officers, Boards, and Committees, 2002
- 1083–1086 Thanks to our Reviewers

DIVISION S-1—SOIL PHYSICS

Inversion of Soil Conductivity Profiles from Electromagnetic Induction Measurements: Theory and Experimental Verification

J. M. H. Hendrickx,* B. Borchers, D. L. Corwin, S. M. Lesch, A. C. Hilgendorf, and J. Schlue

ABSTRACT

Noninvasive electromagnetic (EM) induction techniques are used for salinity monitoring of agricultural lands and contaminant detection in soils and shallow aquifers. This study has four objectives. The first objective is to summarize an earlier linear model of the response of the EM38 ground conductivity meter and to discuss a more accurate nonlinear response model. The second objective is to verify experimentally whether the linear and nonlinear models derived for homogeneous media are valid in heterogeneous soil profiles. The third objective is to present an inverse procedure that combines the nonlinear model with Tikhonov regularization. The fourth objective is the experimental verification of inverse procedures with the linear and nonlinear models for inversion of soil conductivity profiles using aboveground electromagnetic induction measurements on fourteen saline Californian soil profiles. The linear and nonlinear models derived for homogeneous media are indeed valid in heterogeneous soil profiles. However, since the errors of the linear model are approximately double those of the nonlinear model, the latter is the preferred one. A small difference was found in the errors of the inverse procedures between the linear and nonlinear models. In this study, the inverse procedures with the linear model and with the nonlinear model produce equally good solutions at EM38 measurements below 100 mS m⁻¹, while at higher electrical conductivities the inverse procedure with the nonlinear model appears to yield slightly better results. The inverse procedure with the linear model is preferred for all conductivities since it needs considerably less computer resources.

THE NONINVASIVE ELECTROMAGNETIC induction technique is used for salinity monitoring in agricultural lands (Boivin et al., 1988; Cameron et al., 1981; Hendrickx et al., 1992; Job et al., 1987; de Jong et al., 1979; Lesch et al., 1995a, 1995b; Rhoades, 1993; Rhoades et al., 1990b, 1999) and nature reserves (Sheets et al., 1994), detection of contaminants in soils and shallow aquifers (Barker, 1990; Hendrickx et al., 1994; Hoekstra et al., 1992; Ladwig, 1982; Saunders and Cox, 1987; Valentine and Kwader, 1985), soil water content measurements (Kachanoski et al., 1988, 1990; Sheets and Hendrickx, 1995), and vadose zone characterization (Cook et al., 1989; Scanlon et al., 1999). Ground conductivity meters such as the Geonics EM38 (Mississauga, ON, Canada; www.geonics.com) used in this study are relatively inexpensive and easy to use in obtaining EM measurement.

Presently, the EM method appears to be the method of choice for quick characterization of the vadose zone and shallow aquifers. The technique has been proven very successful for detection of lateral changes in the apparent electrical conductivity (EC_a) of soils and shallow groundwater aquifers.

For the detection of vertical EC_a changes in soil profiles from aboveground EM measurements, many investigators have used empirical relations (Cook and Walker, 1992; Corwin and Rhoades, 1982, 1984; Rhoades and Corwin, 1981; Rhoades et al., 1989; Wollenhaupt et al., 1986) and, in one case, theoretical response functions for homogeneous profiles (Slavich, 1990). All of these studies have been based on the assumption of linearity. Rhoades and Corwin (1981) and Slavich (1990) used multiple linear regression to correlate ground conductivity meter EM readings with measured soil electrical conductivity profiles. The resulting coefficients could be used to predict soil electrical conductivity profiles at points where direct measurements were unavailable. Such regression models proved to be site specific. Hence these relations yield reasonable results at the locations for which they have been developed or at locations with similar characteristics, but they cannot be extrapolated to sites with different characteristics without calibration.

McNeil (1980) presented a linear model of the response of the ground conductivity meter. Corwin and Rhoades (1982, 1984) and Cook and Walker (1992) used this model of the ground conductivity meter's response to select linear combinations of measurements that maximized the response to conductivity within a depth range of interest. Borchers et al. (1997) used this same linear model of McNeil (1980) with second order Tikhonov regularization, that is, an inverse procedure, to estimate apparent electrical conductivity profiles. Contrary to the other approaches, Borchers' inverse procedure with the linear model is based solely on electromagnetic physics, which requires no further field calibration.

An important issue is whether the physical equations that describe the electromagnetic response for homogeneous media are valid in heterogeneous field soils. At this moment, it is not entirely clear whether the attempts to use EM measurements for the determination of the vertical distribution of EC_a are only thwarted by the problem of nonuniqueness inherent to inverse procedures or also by a lack of understanding of the physical relationships between the vertical distribution of the

J.M.H. Hendrickx and J. Schlue, Geophysical Research Center and Dep. of Earth & Environmental Science; B. Borchers and A.C. Hilgendorf, Dep. of Mathematics, New Mexico Tech, Socorro, NM 87801; D.L. Corwin and S.M. Lesch, Agricultural Research Service, U.S. George E. Brown Jr. Salinity Laboratory, Riverside, CA 92507-4617. Received 19 July 1999. *Corresponding author (hendrick@nmt.edu).

soil EC_a and the response of the EM ground conductivity meter in heterogeneous field soils. These relationships are expressed quantitatively by the depth response functions which determine the EM response to changes of EC_a with depth. McNeill (1980) presents two depth response functions for the EM ground conductivity meter in, respectively, a horizontal and vertical position. These functions are based on a first-order approximation of the complete physical equations derived by Wait (1982) for a homogeneous half space. McNeill (1980) states without experimental proof that his response functions also apply for heterogeneous soil profiles.

In this paper we summarize a simple linear model and a more complicated nonlinear model of the response of a ground conductivity meter to variations of soil apparent electrical conductivity with depth. We compare the effectiveness of these models in predicting instrument readings. Both the linear and nonlinear models can be used within an inverse procedure to estimate soil apparent electrical conductivity profiles from aboveground EM measurements. We describe our inverse procedures and compare their effectiveness for solving the inverse problem. These overall goals lead to four specific objectives. The first objective is to summarize an earlier linear model of the response of the EM38 ground conductivity meter and to discuss a more accurate nonlinear response model. To our knowledge, this nonlinear model, which has been used widely in frequency domain EM work at greater depths, has not been used with ground conductivity meters operating at the near subsurface. The second objective is to verify experimentally whether the linear and nonlinear models derived by McNeill (1980) and Wait (1982), respectively, for homogeneous media are valid for heterogeneous soil profiles. The third objective is to present an inverse procedure for estimating soil electrical conductivity profiles that combines the nonlinear model with Tikhonov regularization. The fourth objective is the experimental verification of the inverse procedures with the linear (Borchers et al., 1997) and nonlinear (this study) models for inversion of soil conductivity profiles using aboveground electromagnetic induction measurements with a ground conductivity meter.

THEORY

The ground conductivity meter used in this study is the Geonics EM38. The EM38 has two coils on a one-meter-long bar. Alternating current is sent through the transmitter coil. This generates a magnetic field, which in turn causes current to flow in the soil. This current flow generates a secondary magnetic field. The EM38 measures the quadrature component of the ratio of the two magnetic fields. The instrument can be held so that the two coils are oriented horizontally or vertically with respect to the soil surface. For nonuniform electrical conductivity profiles, the instrument will give different readings in these two orientations.

Linear Model of the EM38 Response

In analyzing the response of the EM38, the skin depth δ is of some importance. The skin depth is the depth at

which the primary magnetic field has been attenuated to $1/e$ (i.e., 37%) of its original strength (e is the base of the natural system of logarithm and is ≈ 2.71828). Ground conductivity meters are designed to work with a skin depth that is much larger than the coil spacing. The induction number N_B is defined as the ratio of the intercoil spacing to the skin depth δ (McNeil, 1980; Sharma, 1997; Wait, 1982). For a soil with uniform conductivity σ , it can be shown that

$$N_B = r/\delta = r\sqrt{\mu_0\omega\sigma/2}, \quad [1]$$

where $\mu_0 = 4\pi 10^{-7} \text{ H m}^{-1}$ is the magnetic permeability of free space, σ is the soil conductivity, and ω is the angular operating frequency of the instrument. The EM38 operates at a frequency (f) of 14.6 kHz (i.e., $\omega = 91.7 \times 10^3 \text{ rad s}^{-1}$) with a coil spacing of 1 m. The typical skin depth for the EM38 is 10 to 50 m.

It can be shown (McNeil, 1980; Wait, 1982) that when $N_B \ll 1$, and the instrument is held at the surface, the ratio of the quadrature component of the secondary magnetic field H_s to the primary magnetic field H_p is proportional to the soil conductivity:

$$\text{Im}(H_s/H_p) = \mu_0\omega r^2\sigma/4. \quad [2]$$

The EM38 measures the ratio $\text{Im}(H_s/H_p)$. An apparent conductivity reading m is given by

$$m = \frac{4\text{Im}(H_s/H_p)}{\mu_0\omega r^2}. \quad [3]$$

Note that this apparent conductivity reading is accurate only under the assumptions that the instrument is held at height 0 above the surface, the soil has a uniform conductivity σ , and that $N_B \ll 1$.

A linear model which is based on the assumption that $N_B \ll 1$ but which can be used to predict the response of the instrument at a height h above a soil with depth varying conductivity has been described in McNeil (1980) and Borchers et al. (1997). In this linear model, predictions of the apparent conductivity reading with the coils in the horizontal orientation are given by

$$m^H(h) = \int_0^\infty \phi^H(z+h)\sigma(z)dz. \quad [4]$$

Here the superscript H indicates the horizontal orientation of the coils, h is the height of the instrument above the ground, $\sigma(z)$ gives the conductivity at depth z , and the sensitivity function $\phi^H(z)$ is given by

$$\phi^H(z) = 2 - \frac{4z}{(4z^2 + 1)^{1/2}} \quad [5]$$

Similarly, predictions of the apparent conductivity reading with the coils in the vertical orientation are given by

$$m^V(h) = \int_0^\infty \phi^V(z+h)\sigma(z)dz, \quad [6]$$

where

$$\phi^V(z) = \frac{4z}{(4z^2 + 1)^{3/2}}. \quad [7]$$

In Borchers et al. (1997), a version of this model for layered soil conductivity profiles and measurements at a fixed set of heights was presented. In this layered

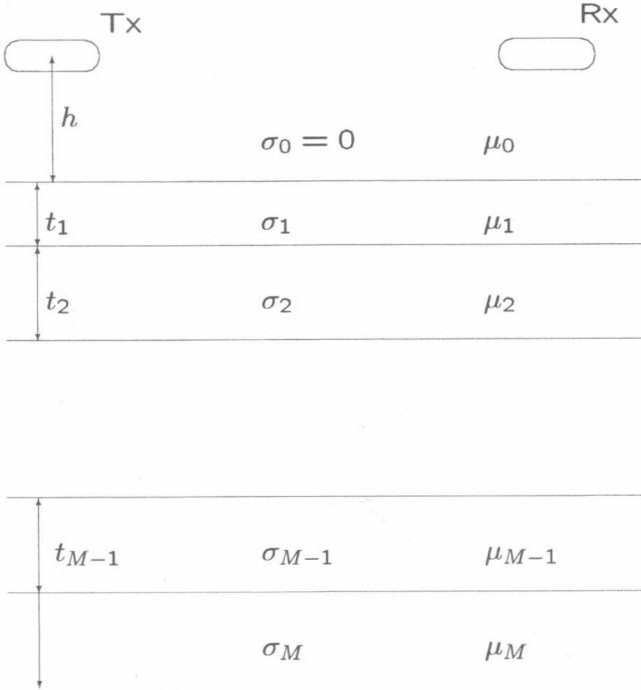


Fig. 1. Schematic of the M -layer model. Rx and Tx represent the receiver and transmitter coil of the noninvasive electromagnetic ground conductivity meter; t is the thickness of the soil layer; σ is the apparent electrical conductivity; σ_0 is the apparent electrical conductivity of free space; μ is the magnetic permeability; μ_0 is the magnetic permeability of free space; h = height; and M is the number of layers including the semi-infinite layer at the bottom.

model, measurements are taken at heights h_1, h_2, \dots, h_n above the soil surface. We assume that the soil has been split into layers with specified thickness, conductivity, and magnetic permeability. Within each layer, the conductivity and magnetic permeability are assumed to be uniform. There are M layers, with the bottom layer, M , extending downward to infinity (Fig. 1). The magnetic permeability of the k th layer is μ_k . In the linear model, we will make the simplifying assumption that the magnetic permeability of the soil is equal to that of free space ($\mu_i = \mu_0$) which is true for most soils. The vector σ will contain the conductivities of the layers. The conductivity of the k th layer is σ_k . The thickness of the k th layer is t_k . We construct a vector containing the predicted apparent conductivity measurements with

$$\mathbf{m}(\sigma) = \begin{bmatrix} m^V(h_1) \\ m^V(h_2) \\ \dots \\ m^V(h_n) \\ m^H(h_1) \\ m^H(h_2) \\ \dots \\ m^H(h_n) \end{bmatrix} \quad [8]$$

With the model of Eq. [4] through [7], $\mathbf{m}(\sigma)$ is given by

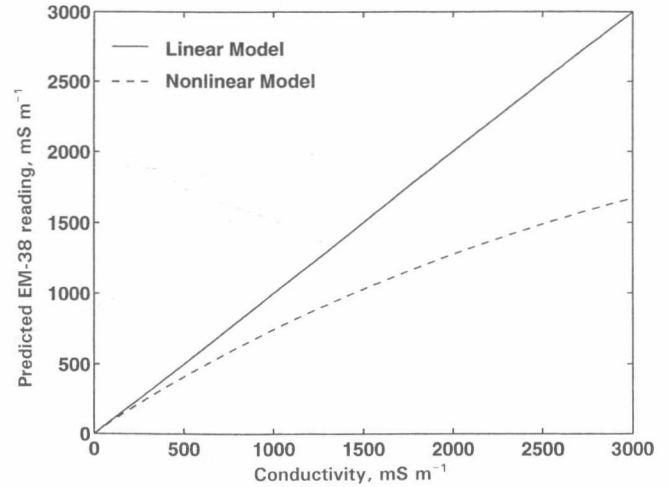


Fig. 2. Linear and nonlinear model predictions of the EM38 measurements with the coils oriented vertically over a soil of uniform conductivity.

$$\mathbf{m}(\sigma) = \mathbf{K}\sigma, \quad [9]$$

where

$$\mathbf{K} = \begin{bmatrix} \int_0^{t_1} \phi^V(z+h_1)dz \dots \int_{t_1+t_2+\dots+t_{M-1}}^{\infty} \phi^V(z+h_1)dz \\ \dots \dots \dots \\ \int_0^{t_1} \phi^V(z+h_n)dz \dots \int_{t_1+t_2+\dots+t_{M-1}}^{\infty} \phi^V(z+h_n)dz \\ \int_0^{t_1} \phi^H(z+h_1)dz \dots \int_{t_1+t_2+\dots+t_{M-1}}^{\infty} \phi^H(z+h_1)dz \\ \dots \dots \dots \\ \int_0^{t_1} \phi^H(z+h_n)dz \dots \int_{t_1+t_2+\dots+t_{M-1}}^{\infty} \phi^H(z+h_n)dz \end{bmatrix} \quad [10]$$

The assumption that $N_B \ll 1$ is critical. Although this assumption is appropriate for soils of relatively low conductivity, the assumption does not hold for soils of medium to high conductivity. For example, consider the response of the EM38 ground conductivity meter with the coils in the vertical orientation, at ground level, over a soil with uniform conductivity. At a true soil conductivity of 10 mS m^{-1} , $N_B = 0.02$, and the response of the instrument predicted by the linear model is 10 mS m^{-1} , while the response predicted by the more accurate nonlinear model presented in this paper is 9.7 mS m^{-1} . At a soil conductivity of 100 mS m^{-1} , $N_B = 0.08$, and the response of the instrument predicted by the linear model is 100 mS m^{-1} , while the nonlinear model predicts a response of 91.9 mS m^{-1} . Figure 2 shows the response of the EM38 as predicted by the linear model and by the nonlinear model. The nonlinearity of the response becomes pronounced at conductivities of $>100 \text{ mS m}^{-1}$. At extremely high conductivities, the instrument can even give negative readings. We have seen this happen when we took readings over a buried iron pipe.

Nonlinear Model of the EM38 Response

A more sophisticated nonlinear model of electromagnetic induction has been widely used in geophysical

work (Wait, 1982; Ward and Hohmann, 1987). This model of the response of the ground conductivity meter is appropriate where the assumption that $N_B \ll 1$ breaks down. Furthermore, this model can be used to predict the apparent conductivity given by Eq. [2] when the soil conductivity varies with depth. As in Borchers et al. (1997), we will again assume that the soil conductivity has a layered structure with M layers as shown in Fig. 1.

In the following discussion, we will make use of two scaling factors which simplify the computations and keep numerical values within a reasonable range. The first scaling factor is $\delta = \sqrt{2/\sigma_1\mu_0\omega}$, with σ_1 equal to the apparent electrical conductivity of layer 1 (see Fig. 1). If the soil conductivity does not vary with depth, δ is the skin depth referred to in Eq. [1]. For general conductivity profiles, δ has no physical significance but is still useful as a scaling factor. A second related scaling factor is $B = r/\delta$.

Maxwell's equations govern the behavior of the electromagnetic fields generated by the ground conductivity meter. It is easier to solve these equations in the frequency domain than in the time domain. If we take a vertical axis through the center of the transmitter coil and consider what happens as we rotate the receiver coil around this vertical axis, we see that the magnetic field sensed by the receiver coil is independent of the rotation of the instrument around this vertical axis. Because of the cylindrical symmetry inherent in this problem, Hankel transforms are used to transform to and from the frequency domain. Thus, the predicted EM38 measurements are expressed in terms of Hankel transforms. In the following, the variables λ and g related by $\lambda = gB/r$ are used as the variables of integration in the Hankel transforms. These variables have no direct physical significance.

The characteristic admittance of the k th layer is denoted by N_k , and is given by

$$N_k = \frac{\sqrt{\lambda^2 + i\sigma_k\mu_k\omega}}{i\mu_k\omega} \quad [11]$$

As in the linear model, σ_k denotes the apparent electrical conductivity of the k th layer, and μ_k denotes the magnetic permeability of the k th layer. The surface admittance at the top of the k th layer is denoted by Y_k . The surface admittances are obtained by solving a set of equations that give the surface admittance of the k th layer as a function of all lower layers (\tanh = hyperbolic tangent):

$$Y_1 = N_1 \frac{Y_2 + N_1 \tanh(u_1 d_1)}{N_1 + Y_2 \tanh(u_1 d_1)}, \quad [12]$$

$$Y_2 = N_2 \frac{Y_3 + N_2 \tanh(u_2 d_2)}{N_2 + Y_3 \tanh(u_2 d_2)}, \quad [13]$$

$$Y_{M-2} = N_{M-2} \frac{Y_{M-1} + N_{M-2} \tanh(u_{M-2} d_{M-2})}{N_{M-2} + Y_{M-1} \tanh(u_{M-2} d_{M-2})}, \quad [14]$$

$$Y_{M-1} = N_{M-1} \frac{N_M + N_{M-1} \tanh(u_{M-1} d_{M-1})}{N_{M-1} + N_M \tanh(u_{M-1} d_{M-1})}, \quad [15]$$

where

$$u_k = \sqrt{\lambda^2 + i\sigma_k\mu_k\omega}. \quad [16]$$

Predicted values of the apparent conductivity measurements $m^V(h)$ (vertical orientation of coils) and $m^H(h)$ (horizontal orientation of coils) at height h above the ground are given by

$$m^V(h) = (4/\mu_0\omega r^2) \text{Im}(1 + B^3 T_0) \quad [17]$$

and

$$m^H(h) = 4/\mu_0\omega r^2 \text{Im}(1 + B^2 T_2) \quad [18]$$

where

$$T_0 = -\int_0^\infty R_0(gB/r) g^2 e^{-2gh/\delta} J_0(gB) dg \quad [19]$$

and

$$T_2 = -\int_0^\infty R_0(gB/r) g e^{-2gh/\delta} J_1(gB) dg \quad [20]$$

Here, $J_0()$ and $J_1()$ are Bessel functions of the first kind of order 0 and 1, respectively (Zwillinger, 1996). $R_0(\lambda)$ is given by

$$R_0(\lambda) = \frac{N_0 - Y_1}{N_0 + Y_1} \quad [21]$$

Inverse Procedure

In this section we discuss a procedure for obtaining estimates of the vector of conductivities σ from a vector d of observations:

$$d = \begin{bmatrix} m_1^V \\ m_2^V \\ \dots \\ m_n^V \\ m_1^H \\ m_2^H \\ \dots \\ m_n^H \end{bmatrix} \quad [22]$$

Here, m_i^V and m_i^H are the actual measurements obtained with the instrument at height h_i , with the coils in the vertical and horizontal orientation, respectively.

An inversion procedure based on the linear model of Eq. [4] through [9] has been described in Borchers et al. (1997). In this section, we generalize the procedure for use with both the linear model of Eq. [4] through [9] and the nonlinear model of Eq. [11] through [21]. Further discussion of the basic procedure can be found in Borchers et al. (1997).

We want to minimize the difference between the observations d and the predicted measurements $m(\sigma)$. Since electrical conductivities are inherently nonnegative, it is also necessary to include nonnegativity constraints in our procedure. We could simply attempt to solve the least squares problem

$$\min \|m(\sigma) - d\|^2, \quad [23]$$

subject to

$$\sigma \geq 0. \quad [24]$$

However, this least squares problem is extremely ill-conditioned. That is, the least squares solution is very sensitive to small amounts of noise in d . Since in practice the EM38 measurements are somewhat noisy, it is necessary to regularize the solution in some way.

In the form of second-order Tikhonov regularization used here (Groetsch, 1993; Hansen, 1997; Tikhonov and Arsenin, 1977), we regularize the solution by solving the modified least squares problem

$$\min \|\mathbf{m}(\sigma) - d\|^2 + \alpha^2 \|L\sigma\|^2, \quad [25]$$

subject to

$$\sigma \geq 0. \quad [26]$$

Here, $L\sigma$ is a finite difference approximation to the second derivative of σ , with

$$L = \begin{bmatrix} 1 & -2 & 1 & & & \\ & 1 & -2 & 1 & & \\ & & & \dots & & \\ & & & & \dots & \\ & & & & & 1 & -2 & 1 \end{bmatrix} \quad [27]$$

The $\alpha^2 \|L\sigma\|^2$ term biases the least squares problem toward solutions in which the conductivity profile is smooth. In the extreme case, $\alpha = 0$, we are simply solving the least squares problem of Eq. [23] and [24]. For larger values of α , we obtain a solution which balances the smoothness of the solution with the norm of the misfit. The parameter α must be chosen carefully to achieve an appropriate balance.

There are a variety of methods for choosing the regularization parameter, including the discrepancy principle (Morozov, 1984), the L-curve criterion (Hansen, 1993), and generalized cross validation (Wahba, 1990). An evaluation of these methods showed that the L-curve criterion worked best for this problem (Hilgendorf, 1997).

If we plot $\|\mathbf{m}(\sigma) - d\|$ vs. $\log \|L\sigma\|$, a characteristic L-shaped curve often appears (Borchers et al., 1997; Hansen, 1992; Lawson and Hanson, 1974). For large values of α we are effectively minimizing $\|L\sigma\|$, while for small values of α , we are effectively minimizing $\|\mathbf{m}(\sigma) - d\|$. Intermediate values of α correspond to solutions near the corner of the curve. Under the L-curve criterion (Hansen, 1992), we pick a value of α that corresponds to the corner of the L-curve. This value can be obtained by manually examining the plot or by an automated procedure (Hansen, 1993) that finds the point on the curve where curvature is maximized.

Our algorithm for obtaining estimates of the conductivities can be summarized as follows:

Step 1. Solve the optimization problem presented in Eq. [25] and [26] for a range of values of α . If the linear model is being used, then use Eq. [4] through [9] to evaluate $\mathbf{m}(\sigma)$. If the nonlinear model is being used, then use Eq. [11] through [21] to evaluate $\mathbf{m}(\sigma)$.

Step 2. Plot the L-curve and find the corner value of α .

Step 3. Solve Eq. [25] and [26] for the selected value of α and then plot the corresponding inverse solution σ .

Implementation

The MATLAB implementation of the inverse procedure for the linear model is discussed in Borchers et al. (1997). We have implemented the inverse procedure using the nonlinear model in a FORTRAN program. Input to this program consists of a set of EM38 measurements and a specification of the layer depths and thicknesses to be used. The program first solves Eq. [25] and [26] for a range of values of α . The program then produces a plot of the corresponding L-curve. An automatic procedure selects an optimal value of α , and the corresponding conductivity profile is then plotted.

The optimization problem of Eq. [25] and [26] is solved by the Levenberg-Marquardt method (Gill et al., 1981). In particular, we use the implementation of the Levenberg-Marquardt method in the DBCLS routine of the International Mathematics and Statistics Library (1991). In solving the optimization problem of Eq. [25] and [26], the most time consuming portion of the program is the calculation of the integrals presented in Eq. [19] and [20]. These integrals are Hankel transforms, which generally cannot be evaluated analytically. Because the integrand is highly oscillatory, standard numerical quadrature approaches are extremely inefficient. Instead, a subroutine developed by Anderson (1979) is used to approximate the Hankel transforms.

MATERIALS AND METHODS

Field Measurements

Fourteen soil profiles were selected in agricultural fields in California. At each site, the soil surface was leveled off, and dry mulch, if present, was removed. This was done to ensure that no electrical insulating material was present at the soil surface to affect the response function of the EM38 ground conductivity meter and to have an accurate reference plane for measuring depth from the soil surface. Seventy-two EM readings were taken at each site: The receiver end of the EM38 was aligned in the four directions of the compass (N, NE, S, and SE) in both the horizontal (EM_H) and vertical (EM_V) coil-mode configurations and at heights of 0, 10, 20, 30, 40, 50, 75, 100, and 150 cm above the soil surface. The EC_a distributions of the soil profile beneath the area of EM measurements was then determined to a depth of 3 m using a Martek SCT four-electrode probe system. Nine measurements of EC_a were made within a 60- by 60-cm square grid at 30-cm intervals at depths of 5, 10, 15, 20, 25, 50, 75, 100, 125, 150, 175, ..., 275, and 300 cm. The readings of the first four depths (5, 10, 15, and 20 cm) were obtained by vertically inserting a Martek bedding-probe through a wooden template down into the soil to the desired depth. EC_a measurements were made in the twelve next deeper depths (25–200 cm) using a Martek Rhoades-probe which was horizontally inserted into the soil to the correct location using various surveying and alignment techniques. In order to access these deeper depths, a large trench was excavated in the E-W direction on the south side of the measurement area using a backhoe. This permitted the sampling personnel to drill and core holes horizontally into the soil profile for insertion of the Rhoades-probe and to identify, measure, and describe the stratigraphy

present in the profile. To sample the depths deeper than 200 cm, all of the soil from the surface down to almost 200 cm beneath the sampled grid area was subsequently removed using the backhoe. The remainder of the soil above the 200-cm depth was removed and leveled by hand with the aid of shovels and surveying techniques. The EC_a values for the 200- to 300-cm depths were then determined using the Rhoades-probe, which was inserted vertically into the soil via a hole prepared with a Lord coring sampler and the sampling template described above. It was not possible in all cases to collect data down to 3 m, for example, when a water table was encountered. In such cases, EC_a readings were taken in saturated soil using the bedding-probe to assign values to the deeper material. Approximately 126 to 144 readings were collected at each site to a depth of at least 2.5 m. These data provide a unique, accurate, and intensive data base of EC_a -profile conditions (ground truth) and corresponding EM readings with which to test the responsiveness of the EM38 ground conductivity meter to heterogeneous soil conditions of EC_a , and to develop and test various interpretive procedures and relations.

Since the linear and nonlinear models and the inverse procedures with these models are one-dimensional, we use in this study mean EC_a values for each depth in the soil profile and mean EM values at each height above the soil surface.

Linear and Nonlinear Models and Inverse Procedures

For the implementation of the models and the inverse procedures with these models, the profile with mean EC_a values at depths of 5, 10, 15, 20, 25, 50, 75, 100, 125, 150, 175, ..., 275, 300 cm was used to interpolate the EC_a values at 10-cm intervals down to 3 m with a semi-infinite layer beginning at the 3-m mark. It is assumed that the conductivity of the semi-infinite layer is the conductivity of the last thin layer.

Using the linear MATLAB code and the nonlinear FORTRAN code, predictions were made for EM38 readings at heights 0, 10, 20, 30, 40, 50, 75, 100, and 150 cm, and inverse EC_a predictions were made at depths 5, 15, 25, ..., 275, 285, and 295 cm.

For the evaluation of the fit between predicted values and actual measurements of electromagnetic induction values above the soil surface and belowground apparent soil electrical conductivities, the following error criterion is used:

Error (%) =

$$\frac{[\sum (\text{predicted measurement} - \text{actual measurement})^2]^{1/2}}{[\sum (\text{actual measurement})^2]^{1/2}} \quad [28]$$

In order to evaluate how well our method works for the prediction of the entire soil apparent electrical conductivity profile, Eq. [28] is used with the predicted and actual measurements at depths 25, 50, 75, ..., 250, 275, and 300 cm to calculate the percentage error. Correlation coefficients calculated in this study are based on the ranks rather than the original error percentages in order to eliminate the effects of nonnormal distributions of error percentages. The measurements of apparent soil electrical conductivities were taken to a depth of 3 m, while the penetration depth of the EM38 is ≈ 1.5 m. Therefore, error percentages for the inverse procedures with the linear and nonlinear models have been evaluated to depths of 1.5 and 3.0 m.

RESULTS AND DISCUSSIONS

Field Measurements

The field measurements at the fourteen sites are representative of a wide range of conditions (Tables 1 and

2). The soil profiles vary from uniform to stratified, water table depths vary from 100 to 300 cm below the soil surface, soil horizons cover the entire textural spectrum from sand to clay, and apparent electrical conductivities range from 0 to 2340 mS m⁻¹. Full soil profile descriptions and all original measurements have been presented in great detail by Rhoades et al. (1990a). Since the presented linear and nonlinear models are one-dimensional, we will mostly deal with the geometric mean apparent electrical conductivity at each depth and the mean electromagnetic induction reading at each height above the soil surface. The reason for using the geometric mean is given below. Figure 3 presents, among other features, the mean average apparent electrical conductivity with depth and its 95% confidence interval for the fourteen sites. The soil profiles cover a wide range of salinity conditions from moderate salinity (Sites 3, 12, and 14) to high salinity (Sites 1, 5, 6, and 7), from a decreasing salinity profile with depth (Site 2) to an increasing one (Site 7), and from smooth salinity profiles (Sites 1, 2, 6, 7, and 14) to rough ones (Sites 3, 4, 5, 8, 9, 10, 11, 12, and 13).

Table 2 summarizes all conductivity measurements taken above the soil surface with the ground conductivity meter EM38 and below it with the Martek Rhoades-probe. A very significant relationship exists between the mean apparent electrical conductivity (EC_a^{mean}) measured with the Rhoades-probe and the mean EM38 measurements at the soil surface in the vertical ($EM38_v^{\text{mean}}$) and horizontal mode ($EM38_h^{\text{mean}}$):

$$EC_a^{\text{mean}} = 1.749 \times EM38_v^{\text{mean}} \quad (R^2 = 0.97; F = 463 \text{ with } P < 0.0001)$$

$$EC_a^{\text{mean}} = 1.487 \times EM38_h^{\text{mean}} \quad (R^2 = 0.94; F = 244 \text{ with } P < 0.0001). \quad [29]$$

Since the effective penetration depth of the EM38_v and EM38_h measurements is ≈ 1.5 m and 0.75 m, respectively, the following relationships have also been determined:

$$EC_a^{\text{mean } 1.5 \text{ m}} = 1.554 \times EM38_v^{\text{mean}} \quad (R^2 = 0.97; F = 467 \text{ with } P < 0.0001)$$

Table 1. Characteristics of the fourteen profiles.

Site	Soil profile	Water table depth cm	Textures in profile†
1	Approximately uniform	300	SIL, S
2	Approximately uniform	225	SL, SIL, S
3	Stratified lenses	275	SL, SICL, L, SIL
4	Substantial stratification	300	SL, S, C, SI, SIL
5	Approximately uniform	275	SI, S
6	Substantial stratification	300	SICL, S, C
7	Substantial stratification	275	SIL, S, C, SICL
8	Substantial stratification	275	L, S, LS, SL
9	Some stratification	275	SIL, S, CL
10	Some stratification	200	CL, S, CL
11	Approximately uniform	100	CL, SIL, S
12	Some stratification	150	C, CL, S
13	Uniform	275	LC
14	Approximately uniform	250	C

† C, Clay; CL, clay loam; L, loam; LS, loamy sand; SI, silt; SIL, silt loam; SIC, silty clay; SICL, silty clay loam; S, sand; SC, sandy clay; SCL, sandy clay loam; SL, sandy loam.

$$EC_a^{\text{mean } 0.75 \text{ m}} = 1.350 \times EM38_h^{\text{mean}}$$

$$(R^2 = 0.96; F = 329 \text{ with } P < 0.0001),$$
[30]

where $EC_a^{\text{mean } 1.5 \text{ m}}$ and $EC_a^{\text{mean } 0.75 \text{ m}}$ are the mean apparent electrical conductivities to depths of 1.5 and 0.75 m, respectively. The regression equations are all highly significant, but taking the mean apparent electrical conductivity to the effective penetration depth tends to enhance the agreement between EC_a and EM measurements. In the vertical and horizontal modes, the regression coefficients decrease toward unity as we move from 1.5 to 0.75 m. The high correlation between measurements taken with the ground conductivity meter and those taken with the Rhoades Probe indicate that the quality of the field measurements is high.

Another important feature of the mean conductivity data is the positive correlation between the standard deviation and the mean for all three variables EC_a^{mean} , $EM38_v$, and $EM38_h$:

$$\text{Std } EC_a = 0.453 \times EC_a^{\text{mean}}$$

$$(R^2 = 0.80; F = 52 \text{ with } P < 0.0001)$$

$$\text{Std } EM38_v = 0.020 \times EM38_v^{\text{mean}}$$

$$(R^2 = 0.62; F = 21 \text{ with } P < 0.0001)$$

$$\text{Std } EM38_h = 0.024 \times EM38_h^{\text{mean}}$$

$$(R^2 = 0.90; F = 114 \text{ with } P < 0.0001).$$
[31]

The increase of the standard deviation with the mean conductivity indicates that the original data have approximately a log-normal distribution, which is a common occurrence for electrical conductivity measurements (Hendrickx et al., 1992). For statistical testing that assumes a normally distributed data set, the logarithms of the original measurements should be used. Since the data are approximately log-normally distributed, we use in this study the geometric means of the apparent electrical conductivities at each depth.

The standard deviation of the EM38 measurements is one to two orders of magnitude smaller than the one of the Rhoades-probe measurements (Table 2). This is most likely caused by the fact that the measurement volume of the EM38 ground conductivity meter is much larger than that of the Rhoades-probe: $\approx 10^5 \text{ cm}^3$ vs. 10^3 cm^3 . The relatively low variability and robustness of EM38 measurements make the ground conductivity meter a promising tool for inverse procedures.

Linear and Nonlinear Models

Applying error criterion Eq. [28] to the predictions of the EM38 readings using the EC_a measurements with the Martek SCT four-electrode probe in the linear and nonlinear models yields the error percentages presented in Table 2. With only one exception, the predictions with the nonlinear model in horizontal and vertical modes are closer to the actual EM38 measurements than the predictions with the linear model. The only exception is found at Site 4, where the error of the horizontal mode increases from 4% with the linear model to 7% with the nonlinear model; both percentages are among the lowest, which indicates that both models perform well at this site. The mean error percentage for horizontal and vertical mode decreases from 38 to 18% and from 55 to 21%, respectively, when the linear model is replaced by the nonlinear one. As an illustration, Fig. 4 presents the two worst cases (Sites 13 and 8) and two regular cases (Sites 6 and 5) of predictions with the linear and nonlinear models. At most sites the nonlinear model yields predictions that coincide closely with the field measurements taken by the ground conductivity meter.

Significant rank correlation coefficients of 61% ($P < 0.05$) and 62% ($P < 0.01$) are found between the mean apparent electrical conductivity in the top 1.5 m of the soil profile and the error percentages in the horizontal and vertical linear models, respectively. Thus, errors increase with increasing salinity when the assumption of linearity is no longer warranted. No such correlation

Table 2. Geometric means.

Site		Mean electrical conductivity measured at soil surface using EM38				Apparent electrical conductivity measured in top 1.5 m of soil profile using Rhoades Probe					Error							
		Vertical mode		Horizontal mode		Number of measurements					linear model		nonlinear model		Inverse procedure with			
															linear model		nonlinear model	
		Mean	Std	Mean	Std						Mean	Std	Min	Max	H	V	H	V
mS m ⁻¹																		
1	smooth	553	9	580	8	90	828	192	405	1210	34	53	15	19	39	27	71	26
2	smooth	179	6	290	11	90	373	330	45	1510	20	21	19	18	46	46	34	34
3	rough	84	2	73	3	90	99	59	19	241	27	39	14	21	25	26	25	28
4	rough	111	1	163	5	90	169	116	4	546	4	5	7	2	34	25	32	28
5	rough	641	25	833	17	90	1173	430	400	2340	61	93	23	18	67	34	25	28
6	smooth	463	3	581	15	90	574	218	206	1190	52	91	6	4	75	26	20	23
7	smooth	420	0	288	3	90	419	444	15	1340	96	124	7	3	79	31	17	23
8	rough	268	13	336	9	90	436	192	18	879	65	109	32	46	77	38	67	36
9	rough	106	4	132	5	90	177	53	40	285	18	35	14	28	39	30	43	39
10	rough	362	1	408	16	90	417	186	35	886	7	14	4	4	34	27	33	29
11	rough	375	6	441	12	81	686	202	327	1030	43	49	33	29	32	32	32	32
12	rough	91	1	62	1	90	117	117	0	320	30	32	27	28	40	40	41	41
13	rough	119	1	129	4	90	204	47	119	337	56	79	42	54	40	32	38	31
14	smooth	68	1	59	4	90	82	40	20	193	13	21	9	13	44	35	39	37
Mean error percentage											38	55	18	21	48	32	37	31

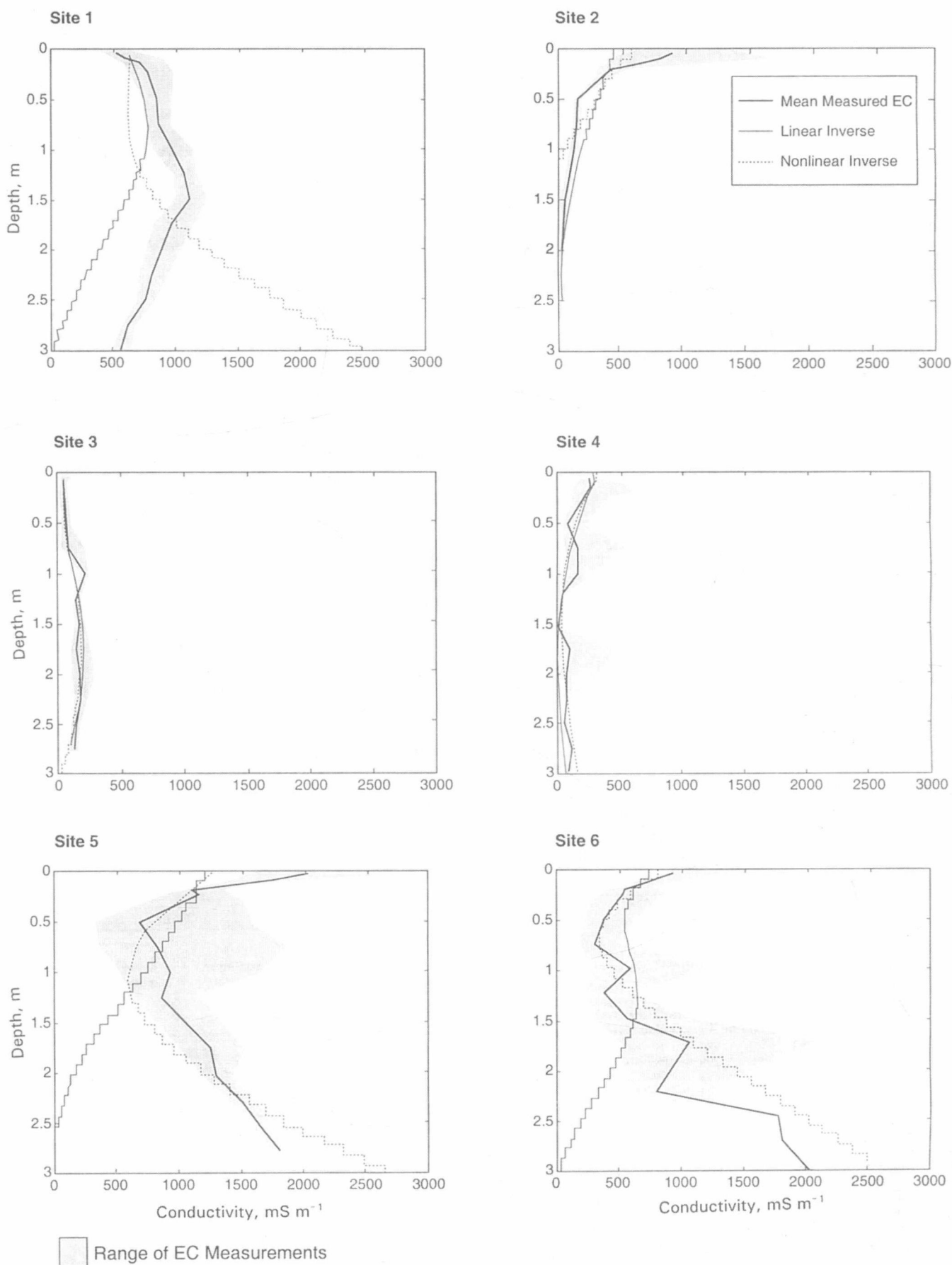


Fig. 3. Continued on next page.

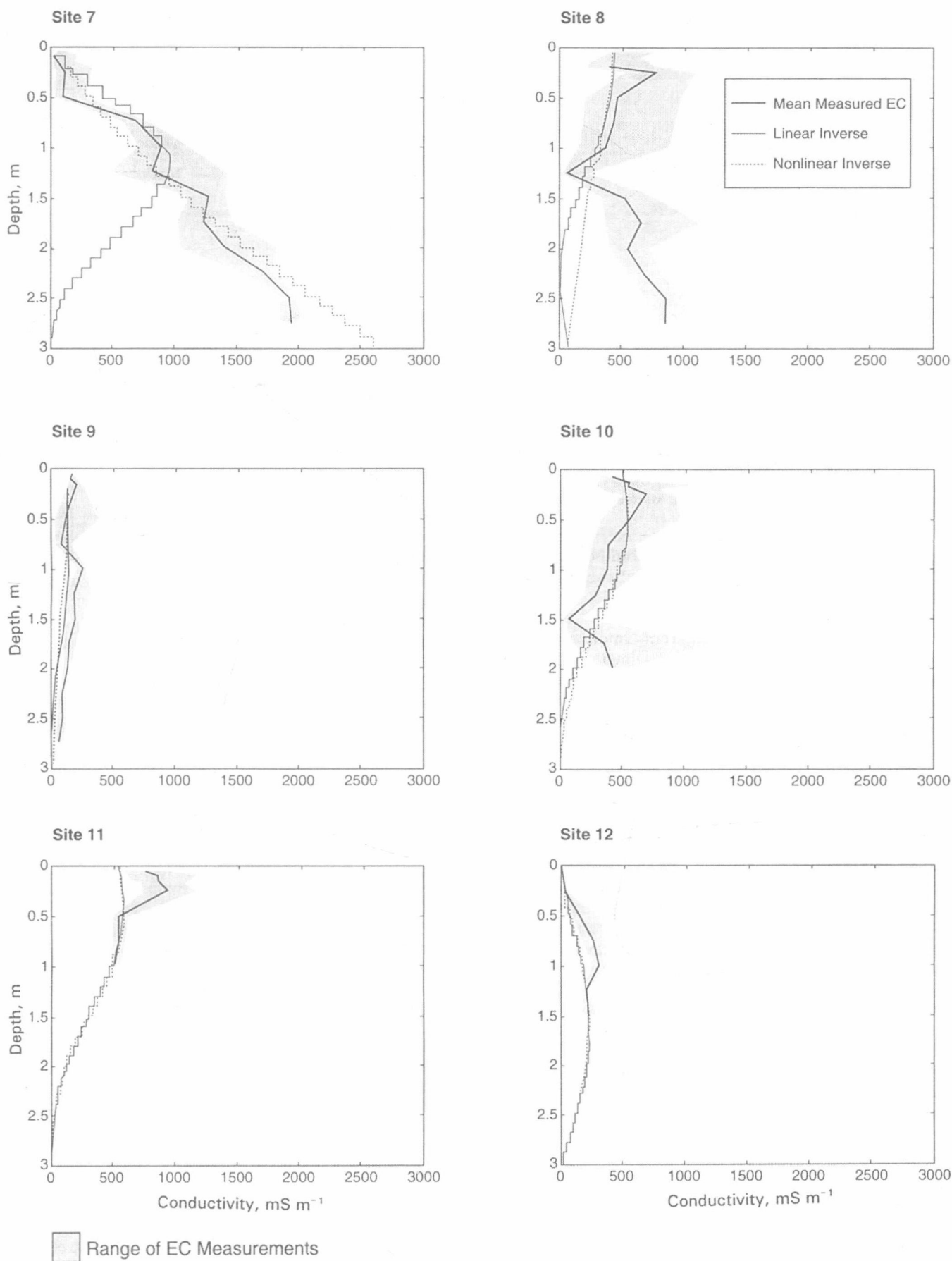


Fig. 3. Continued on next page.

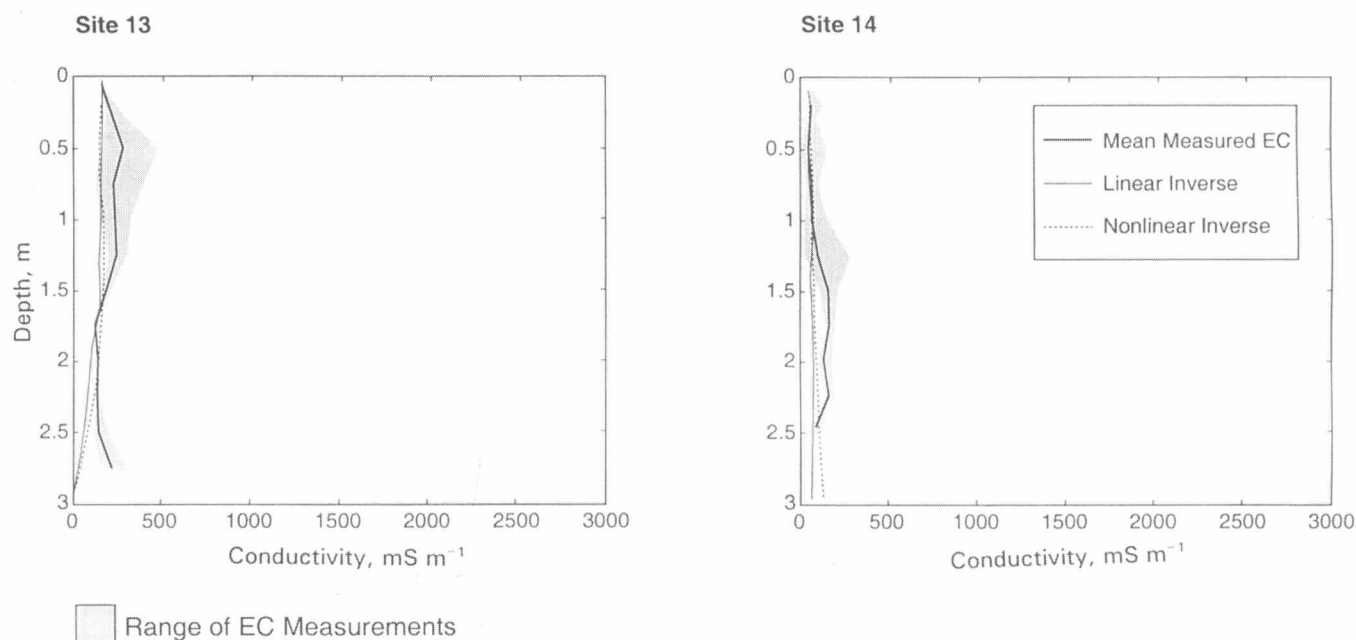


Fig. 3. Depth profiles of mean measured apparent soil electrical conductivity EC , its range, and the predictions from the inverse procedures with the linear and nonlinear models in fourteen soil profiles.

is found between the mean apparent electrical conductivity and the (smaller) errors for the nonlinear models, which again confirms the superiority of the nonlinear over the linear model as a more complete physical model.

Even for the lowest mean apparent conductivities or lowest mean EM38 measurements, the linear model may result in considerable errors (Table 2). For example, at Site 14 with a mean apparent conductivity of 82 mS m^{-1} , the errors of the linear horizontal and vertical models are 13 and 21%, which improve to 9 and 13% when the nonlinear model is employed. A similar effect is found at the other low salinity site, Site 3. Both these sites have maximum salinity values of 193 and 241 mS m^{-1} , respectively. Apparently, it takes only a few layers in a soil profile with a conductivity higher than 100 mS m^{-1} to compromise the response of the instrument.

In Table 2 we make a (subjective) distinction between profiles with a *smooth* and a *rough* apparent electrical conductivity profile. A *t*-test determined that for the nonlinear horizontal and vertical models, the mean error percentage of the rough profiles is significantly larger ($P < 0.05$) than for the smooth profiles. The difference was 22 and 26% for the horizontal and vertical EM38 predictions in the rough profiles, respectively, vs. 11 and 11% in the smooth profiles. Thus, the one-dimensional nonlinear models used in this study perform less satisfactorily when confronted with an increased variability in soil apparent electrical conductivity. One reason may be that the larger variability results in a less reliable estimate of the mean apparent electrical conductivity at each depth and, consequently, leads to a less reliable prediction of EM38 measurements. Another reason may be that the one-dimensional model is not a good predictor of the three-dimensional behavior of electrical and magnetic fields in a variable soil.

Table 2 and Fig. 4 present evidence that the nonlinear model yields in most of our fourteen soil profiles reliable predictions of apparent electrical conductivity measurements taken with the EM38 ground conductivity meter in heterogeneous soil profiles. This experimental confirmation of the geophysical theory derived by Wait (1982) and McNeill (1980) is not only of academic interest but has important practical implications. First of all, it justifies our exploration of inverse procedures for the prediction of profiles of apparent electrical conductivity with depth using only aboveground EM38 measurements. Secondly, it allows practitioners to assess the sensitivity of an EM survey before going to the field since the linear and nonlinear models can be used to evaluate the minimum salinity change or the minimum concentration of contaminants in the soil water or shallow aquifer that can be detected using EM measurements.

Inverse Procedures with the Linear and Nonlinear Models

Figure 3 presents the predictions of the inverse procedures with the linear and nonlinear models derived by Borchers et al. (1997; this study) for the fourteen electrical conductivity profiles. Visual inspection reveals that the agreement between EC_a measurements and predictions is generally quite good to a depth of 1.5 m. In most cases, the predictions are within the 95% confidence limits. The inverse procedure detects well the overall level of electrical conductivity. For example, compare Site 1 (high) with Sites 3 and 14 (low). In addition, the shape of the electrical conductivity with depth often is detected as can be seen in Sites 3, 7, and 12 (increasing with depth), Sites 2, 4, 8, and 10 (decreasing with depth), Sites 9, 13, and 14 (little change with depth), and Sites 5 and 6 (bulging profile).

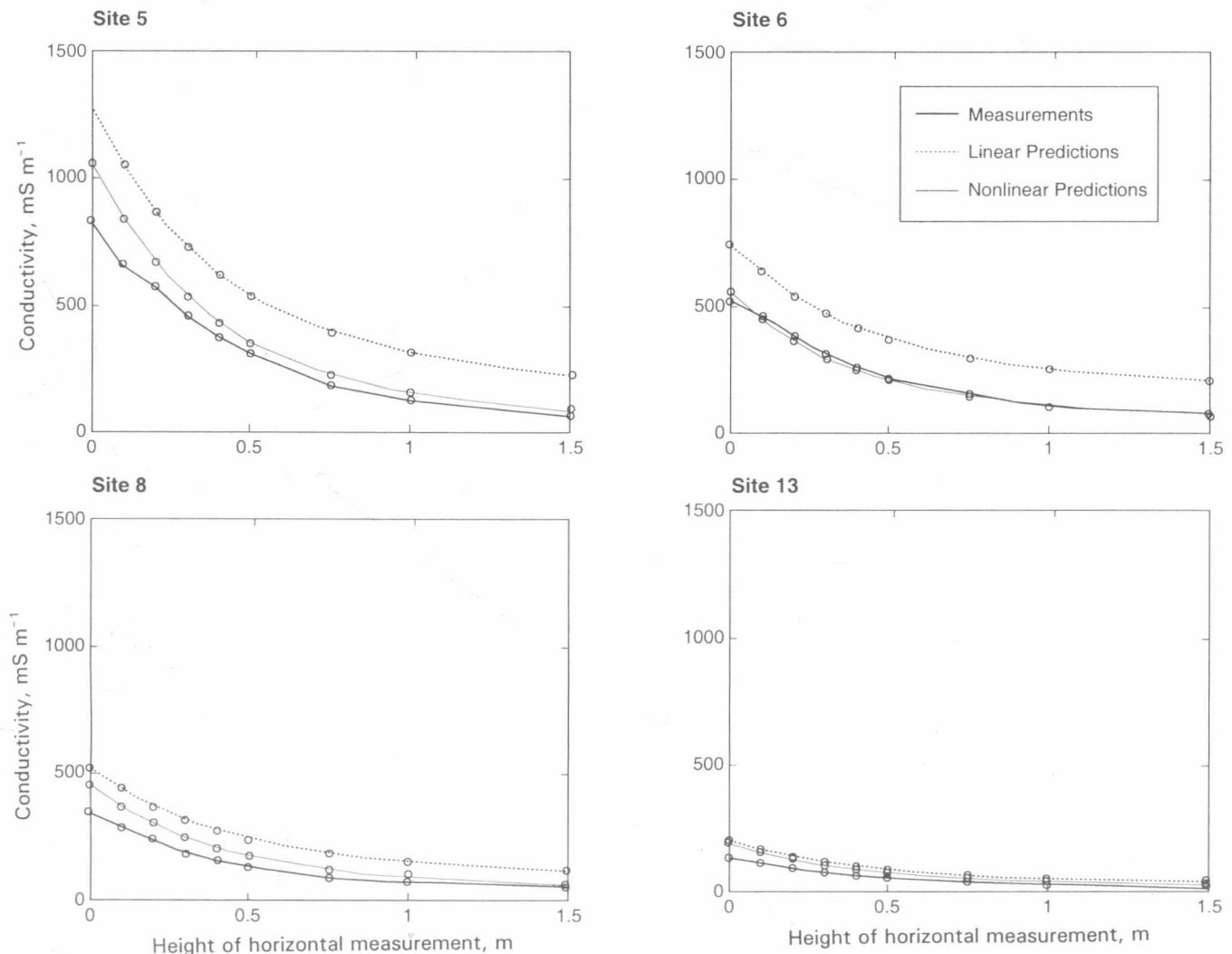


Fig. 4. Mean apparent soil electrical conductivities measured with the EM38 ground conductivity meter in vertical mode at different heights above the soil surface and their predictions with the linear and nonlinear models for four representative profiles.

A more formal method to evaluate the inverse solutions is the application of error criterion in Eq. [28], which yields the error percentages presented in Table 2. With few exceptions, the predictions for the 1.5-m-deep soil profile result in less error than those for the 3.0-m-deep soil profile. The mean error percentages for the linear and nonlinear predictions to a depth of 3.0 m are 48 and 37%, respectively, which is larger than the mean error percentages of 32 and 31% for predictions to a depth of 1.5 m. This result reflects the effective penetration depth of the EM38 ground conductivity meter, which is ≈ 1.5 m. Therefore, only the results for the 1.5-m-deep soil profiles will be considered below.

A salient feature of Table 2 is the large difference in error percentage between the linear and nonlinear models. In the horizontal mode the difference is $38 - 18 = 20\%$, while in the vertical mode it is $55 - 21 = 34\%$. Yet, the difference in error percentage between the inverse procedures with the linear and nonlinear inverse models using 1.5-m-depth is very small, as it amounts to $32 - 31 = 1\%$. Although the nonlinear model yields better predictions than the linear model,

inverse procedures based on the linear and nonlinear models do about as well. The magnitude of the errors in the inverse solutions depends in a complicated way on the measurement noise, errors in the linear and nonlinear models, and bias introduced by Tikhonov regularization. It appears that, in practice, the effect of errors in the linear and nonlinear models is not as great as the effect of other sources of error in the inverse solution.

Although inverse solutions cannot be used to make highly accurate predictions of soil apparent electrical conductivity profiles, Table 2 demonstrates that it is generally possible to obtain estimates of apparent electrical conductivity to a depth of 1.5 m with an accuracy of $\pm 40\%$. It appears also possible to determine whether the soil electrical conductivity profile is increasing, decreasing, or more or less uniform with depth (Fig. 3). The inverse solutions are often within or close to the 95% confidence limits of the measured soil apparent electrical conductivity. This indicates that the uncertainty in the measured electrical conductivities due to spatial variability is often of the same order of magnitude or larger than the inaccuracy in the inverse solutions.

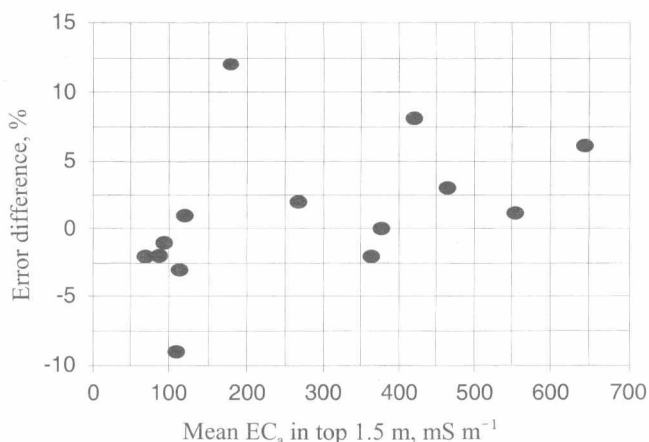


Fig. 5. Mean apparent soil electrical profile conductivity measured with EM38 ground conductivity meter in vertical mode vs. the difference of the errors resulting from the inverse procedures with the linear and nonlinear 1.5-m-depth models.

Figure 5 presents the error differences between the inverse procedures with the linear and nonlinear models vs. mean apparent electrical conductivities in the profile. For sites with a relatively low mean electrical conductivity ($<100 \text{ mS m}^{-1}$ using the EM38 ground conductivity meter), the linear and nonlinear inverse solutions produce essentially the same predictions. One exception is Site 9, where the automatic procedure used to pick the optimal regularization parameter picked a poor value of the regularization parameter for the nonlinear inverse solution. A much better solution can be obtained by picking the regularization parameter by hand. However, in this study we only used the automatic procedure to exclude subjective judgements and bias in the inverse procedure. For sites with a relatively high mean electrical conductivity (more than 400 mS m^{-1} using the EM38 ground conductivity meter), the inverse procedure with the nonlinear model consistently seems to yield slightly more accurate predictions. However, there are many other sources of error in the inverse solution, and the improved accuracy of the nonlinear model seems to have only a small effect.

The inverse results presented in Fig. 3 and Table 2 suggest the following guidelines for the practitioner: Because the inverse procedures with the linear and nonlinear models in this study perform almost equally well across a wide range of electrical conductivity values, the inverse procedure with the linear model is preferred since it takes no more than a few minutes of computer time, while the inverse procedure with the nonlinear model takes 3 to 5 h on a Sun Ultra 1 workstation. The case studies with low EM38 values presented by Borchers et al. (1997) confirm this finding.

SUMMARY

We have described a nonlinear model for the response of a ground conductivity meter to electrical conductivity depth profiles. Unlike a previous linear model, this nonlinear model does not require the induction number to be far less than one. Thus, this model is applicable to measurements of soils of relatively high soil apparent

electrical conductivity. We have also described a procedure that uses this nonlinear model in the inversion of electrical conductivity depth profiles from aboveground EM measurements.

The experimental data from fourteen representative saline soil profiles in California obtained by Rhoades et al. (1990a) have been used for an experimental verification of the linear and nonlinear models and the inverse procedures with the linear and nonlinear models. The linear and nonlinear models derived for homogeneous media (McNeill, 1980; Wait, 1982) are indeed valid in heterogeneous soil profiles. However, since the errors of the linear model are approximately double those of the nonlinear model, the latter is the preferred one.

No such difference was found between the inverse procedures with the linear and nonlinear models. At best, the inverse procedure with the nonlinear model provides a small improvement at higher apparent electrical conductivities. The inverse procedure with the linear model is preferred since it needs considerably less computer resources.

The inverse procedures with the linear and nonlinear models presented by Borchers et al. (1997) and in this study are a valuable tool for noninvasive assessment of soil electrical conductivity depth profiles. Under conditions of relatively low electrical conductivity ($<100 \text{ mS m}^{-1}$), the inverse procedure with the linear model works well. Under conditions of relatively high electrical conductivity, the inverse procedure with the linear model still produces adequate solutions, although the inverse procedure with the nonlinear model may produce slightly better solutions.

ACKNOWLEDGMENTS

This study would not have been possible without funding granted to the senior author by the Waste-Management Education and Research Consortium (WERC) and the Cooperative State Research Service of the USDA.

REFERENCES

- Anderson, W.L. 1979. Computer program numerical integration of related Hankel transforms of order 0 and 1 by adaptive digital filtering. *Geophysics* 44:1287-1305.
- Barker, R.D. 1990. Investigation of groundwater salinity by geophysical methods. p. 201-211. In S.H. Ward (ed.) *Geotechnical and environmental geophysics*. Vol. 2. Soc. of Exploration Geophysicists, Tulsa, OK.
- Boivin, P., D. Brunet, and J.O. Job. 1988. Conductivimétrie électromagnétique et cartographie automatique des sols salés; une méthode rapide et fiable. (In French.) *Cah. ORSTOM, Sér. Pedol.*, 24:1:39-48.
- Borchers, B., T. Uram, and J.M.H. Hendrickx. 1997. Tikhonov regularization of electrical conductivity depth profiles in field soils. *Soil Sci. Soc. Am. J.* 61:1004-1009.
- Cameron, D.R., E. de Jong, D.W.L. Read, and M. Oosterveld. 1981. Mapping salinity using resistivity and electromagnetic techniques. *Can. J. Soil Sci.* 61:67-78.
- Cook, P.G., M.W. Hughes, G.R. Walker, and G.B. Allison. 1989. The calibration of frequency-domain electromagnetic induction meters and their possible use in recharge studies. *J. Hydrol.* 107:251-265.
- Cook, P.G., and G.R. Walker. 1992. Depth profiles of electrical conductivity from linear combinations of electromagnetic induction measurements. *Soil Sci. Soc. Am. J.* 56:1015-1022.
- Corwin, D.L., and J.D. Rhoades. 1982. An improved technique for determining soil electrical conductivity—Depth relations from

- above-ground electromagnetic measurements. *Soil Sci. Soc. Am. J.* 46:517–520.
- Corwin, D.L., and J.D. Rhoades. 1984. Measurement of inverted electrical conductivity profiles using electromagnetic induction. *Soil Sci. Soc. Am. J.* 48:288–291.
- Gill, P.E., W. Murray, and M.H. Wright. 1981. *Practical optimization*. Academic Press, New York.
- Groetsch, C.W. 1993. *Inverse problems in the mathematical sciences*. Vieweg, Wiesbaden, Germany.
- Hansen, P.C. 1992. Analysis of discrete ill-posed problems by means of the L-curve. *SIAM Rev.* 34:561–580.
- Hansen, P.C. 1997. Rank-deficient and discrete ill-posed problems: numerical aspects of linear inversion. SIAM, Philadelphia.
- Hendrickx, J.M.H., B. Baerends, Z.I. Raza, M. Sadiq, and M. Akram Chaudhry. 1992. Soil salinity assessment by electromagnetic induction of irrigated land. *Soil Sci. Soc. Am. J.* 56:1933–1941.
- Hendrickx, J.M.H., C.D. Grande, B.A. Buchanan, and R.E. Bretz. 1994. Electromagnetic induction for restoration of saline environments in New Mexico. p. 247–265. *In* R.K. Bhada et al. (ed.) *Waste management: From risk to remediation*. ECM Series on Environmental Management & Intelligent Manufacturing. Vol. I. ECM Press, Albuquerque, NM.
- Hilgendorf, A. 1997. Linear and nonlinear models for inversion of electrical conductivity profiles in field soils from EM38 measurements. M.S. thesis. New Mexico Inst. of Mining and Technol., Socorro, NM.
- Hoekstra, P., R. Lahti, J. Hild, C.R. Bataes, and D. Phillips. 1992. Case histories of shallow time domain electromagnetics in environmental site assessment: Case history mapping migration of oil field brines from evaporation pits and ponds. *Ground Water Monit. Rev.* 13: 110–117.
- International Mathematics and Statistics Library. 1991. *FORTAN subroutines for mathematical applications*. IMSL, Houston, TX.
- Job, J.O., J.Y. Loyer, and M. Ailoul. 1987. Utilisation de la conductivité électromagnétique pour la mesure directe de la salinité des sols. (In French.) *Cah. ORSTOM, Sér. Pedol.*, 23:2:123–131.
- de Jong, E., A.K. Ballantyne, D.R. Cameron, and D.W.L. Read. 1979. Measurement of apparent electrical conductivity of soils by an electromagnetic induction probe to aid salinity surveys. *Soil Sci. Soc. Am. J.* 43:810–812.
- Kachanoski, R.G., E.G. Gregorich, and I.J. Van Wesebeeck. 1988. Estimating spatial variations of soil water content using non-contacting electromagnetic inductive methods. *Can. J. Soil Sci.* 68:715–722.
- Kachanoski, R.G., E. de Jong, I.J. Van Wesebeeck. 1990. Field scale patterns of soil water storage from non-contacting measurements of bulk electrical conductivity. *Can. J. Soil Sci.* 70:537–541.
- Ladwig, K.J. 1982. Electromagnetic induction methods for monitoring acid mine drainage. *Ground Water Monit. Rev.* 3:46–52.
- Lawson, C.L., and R.J. Hanson. 1974. *Solving least squares problems*. Prentice-Hall, Englewood Cliffs, NJ.
- Lesch, S.M., D.J. Strauss, and J.D. Rhoades. 1995a. Spatial prediction of soil salinity using electromagnetic induction techniques: 1. Statistical prediction models: A comparison of multiple linear regression and cokriging. *Water Resour. Res.* 31:373–386.
- Lesch, S.M., D.J. Strauss, and J.D. Rhoades. 1995b. Spatial prediction of soil salinity using electromagnetic induction techniques: 2. An efficient spatial sampling algorithm suitable for multiple linear regression model identification and estimation. *Water Resour. Res.* 31:387–398.
- McNeill, J.D. 1980. Electromagnetic terrain conductivity measurement at low induction numbers. Tech. Note TN-6. Geonics, ON, Canada.
- Morozov, V.A. 1984. *Methods for solving incorrectly posed problems*. Springer-Verlag, New York.
- Rhoades, J.D. 1993. Electrical conductivity methods for measuring and mapping soil salinity. *Adv. Agron.* 49:201–251.
- Rhoades, J.D., and D.L. Corwin. 1981. Determining soil electrical conductivity—Depth relations using an inductive electromagnetic soil conductivity meter. *Soil Sci. Soc. Am. J.* 45:255–260.
- Rhoades, J.D., D.L. Corwin, and S.M. Lesch. 1990a. Effect of soil EC_a—Depth profile pattern on electromagnetic induction measurements. Res. Rep. 125. USDA-ARS, U.S. Salinity Laboratory, Riverside, CA.
- Rhoades, J.D., D.L. Corwin, and S.M. Lesch. 1999. p. 197–216. *In* D.L. Corwin et al. (ed.) *Assessment of non-point source pollution in the vadose zone*. Geophysical Monogr. 108. American Geophysical Union, Washington, DC.
- Rhoades, J.D., S.M. Lesch, P.J. Shouse, and W.J. Alves. 1989. New calibrations for determining soil electrical conductivity—Depth relations from electromagnetic measurements. *Soil Sci. Soc. Am. J.* 53:74–79.
- Rhoades, J.D., P.J. Shouse, W.J. Alves, N. A. Manteghi, and S.M. Lesch. 1990b. Determining soil salinity from soil electrical conductivity using different models and estimates. *Soil Sci. Soc. Am. J.* 54:46–54.
- Saunders, W.R., and S.A. Cox. 1987. Use of an electromagnetic induction technique in subsurface hydrocarbon investigations. p. 585–599. *In* Proc. Natl. Outdoor Action Conf. on Aquifer Restoration, Ground Water Monitoring and Geophysical Methods, 1st, Las Vegas, NV. 18–21 May 1987. Water Well Journal Publishing Co., Dublin, OH.
- Scanlon, B.R., J.G. Paine, and R.S. Goldsmith. 1999. Evaluation of electromagnetic induction as a reconnaissance technique to characterize unsaturated flow in an arid setting. *Ground Water* 37:296–304.
- Sharma, P.V. 1997. *Environmental and engineering geophysics*. Cambridge Univ. Press, New York.
- Sheets, K.R., and J.M.H. Hendrickx. 1995. Non-invasive soil water content measurement using electromagnetic induction. *Water Resour. Res.* 31:2401–2409.
- Sheets, K.R., J.P. Taylor, and J.M.H. Hendrickx. 1994. Rapid salinity mapping by electromagnetic induction for determining riparian restoration potential. *Restor. Ecol.* 2:242–246.
- Slavich, P.G. 1990. Determining EC_a depth profiles from electromagnetic induction measurements. *Aust. J. Soil Res.* 28:443–452.
- Tikhonov, A.N., and V.Y. Arsenin. 1977. *Solution of ill-posed problems*. John Wiley and Sons, New York.
- Valentine, R.M., and T. Kwader. 1985. Terrain conductivity as a tool for delineating hydrocarbon plumes in a shallow aquifer—A case study. p. 52–63. *In* Proc. Natl. Water Well Assoc. Conf. on Surface and Borehole Geophysical Methods in Ground Investigations, Fort Worth, TX. 12–14 Feb. 1985. National Water Well Publishing Co., Dublin, OH.
- Wahba, G. 1990. *Spline models for observational data*. Society for Industrial and Applied Mathematics, Philadelphia.
- Wait, J.R. 1982. *Geo-Electromagnetism*. Academic Press, New York.
- Ward, S.H., and G.W. Hohmann. 1987. Electromagnetic theory for geophysical applications. p. 131–312. *In* M.N. Nabighian (ed.) *Electromagnetic methods in applied geophysics*. Soc. of Exploration Geophysicists, Tulsa, OK.
- Wollenhaupt, N.C., J.L. Richardson, J.E. Foss, and E.C. Doll. 1986. A rapid method for estimating weighted soil salinity from apparent soil electrical conductivity measured with an above ground electromagnetic induction meter. *Can. J. Soil Sci.* 66:315–321.
- Zwillinger, D. 1996. *Standard mathematical tables and formulae*. 30th ed. CRC Press, Boca Raton, FL.